

OXIDATION BEHAVIOR OF CARBON-SILICON AND CARBON-BORON-SILICON ALLOYS DERIVED FROM SOLVENT-SOLUBLE SILICON AND BORON-SILICON-DOPED COAL-TAR PITCHES

VEDENJE PRI OKSIDACIJI OGLJIK-SILICIJEVIH IN OGLJIK-BOR-SILICIJEVIH ZLITIN, PRIDOBLENJIH IZ RAZTOPIN PREMOGOVE KATRANSKE SMOLE, DOPIRANE S TOPNIM SILICIJEM IN BOR-SILICIJEM

Xiaohua Zuo^{1,2}, Zhijun Dong¹, Wen Li², Guangming Yuan¹, Zhengwei Cui¹, Yue Liu¹, Xuanke Li¹

¹Hubei Province Key Laboratory of Coal Conversion & New Carbon Materials, Wuhan University of Science and Technology, 430081 Wuhan, China

²School of Chemistry & Materials Engineering, Hubei Polytechnic University, 435003 Huangshi, China
xkli@21cn.com

Prejem rokopisa – received: 2013-03-14; sprejem za objavo – accepted for publication: 2013-04-24

The solvent-soluble silicon (Si) and boron-silicon (B-Si) doped coal-tar pitches were synthesized with the co-pyrolysis of a mixture of the toluene-soluble fraction of the coal-tar pitch (TSP), polycarbosilane and pyridine borane. The C-Si and C-B-Si alloys were obtained with a carbonization treatment of the synthetic Si and B-Si doped coal-tar pitches at 1000–1600 °C for 1 h. The physical properties of the Si and B-Si doped coal-tar pitches, such as the softening point, quinoline insolubles, the volatile content and the pyrolysis yield were determined. The influences of the pyridine-borane content in raw materials and the carbonization temperature on the composition, microstructure and oxidation resistance of the C-Si and C-B-Si alloys were investigated. The results show that the C-B-Si alloys are composed of SiC, B₂O₃ and carbon, while the silicon, boron and oxygen elements are uniformly dispersed in the carbon matrix. In most cases, the oxidation resistance of the C-B-Si alloy is better than that of the C-Si alloy, owing to the sintering-aiding action of B₂O₃ and the anti-oxidation synergism of the SiO₂ and B₂O₃ formed during oxidation. The higher the carbonization temperature, the larger is the grain size of the SiC in the C-B-Si alloy. A large grain size leads to an increase in the initial oxidation temperature of the SiC, which is unfavorable for the formation of a protective glassy film on the surface of the C-B-Si alloys. As a result, the C-B-Si alloy obtained with the carbonization at 1200 °C shows a better oxidation resistance than that obtained with the carbonization at 1600 °C under the same oxidation conditions.

Keywords: C-Si alloy, C-B-Si alloy, doped coal-tar pitch, oxidation resistance

Topila premoške katranske smole, dopirane s topnim silicijem (Si) in bor-silicijem (B-Si), so bila sintetizirana s kopirolozo mešanice v toluenu tope frakcije premoške katranske smole (TSP), polikarbosilana in piridin borana. Zlitine C-Si in C-B-Si so bile dobljene s karbonizacijsko obdelavo premoške katranske smole, dopirane s sintetičnim Si in B-Si 1 h pri 1000–1600 °C. Določene so bile fizikalne lastnosti premoške katranske smole, dopirane s Si in B-Si, točka mehčanja, trdni delci ogljika, vsebnost hlapnih snovi in izkoristek pirolize. Preiskovan je bil vpliv vsebnosti piridin borana v surovini in karbonizacijska temperatura na sestavo, mikrostrukturo in oksidacijsko odpornost zlitin C-Si in C-B-Si. Rezultati kažejo, da so zlitine C-B-Si sestavljene iz SiC, B₂O₃ in ogljika, pri čemer so elementi ogljik, silicij, bor in kisik enakomerno razpršeni po osnovi iz ogljika. Odpornost proti oksidaciji je v večini primerov pri zlitini C-B-Si boljše od zlitine C-Si zaradi dodatnega učinka B₂O₃ in protioksidacijske sinergije SiO₂ in B₂O₃, ki nastajata med oksidacijo. Čim višja je temperatura karbonizacije, tem večja postajajo zrna zlitine SiC in C-B-Si. Večja kristalna zrna povzročijo povišanje temperature začetka oksidacije SiC, kar je neugodno za nastanek steklaste zaščitne plasti na površini zlitin C-B-Si. Rezultat tega je, da zlitina C-B-Si, dobljena pri karbonizaciji pri 1200 °C, pri enakih razmerah za oksidacijo kaže boljšo odpornost proti oksidaciji kot zlitina, pridobljena s karbonizacijo pri 1600 °C.

Ključne besede: zlitina C-Si, zlitina C-B-Si, dopirana premoška katranska smola, odpornost proti oksidaciji

1 INTRODUCTION

Carbon materials, particularly in fiber and composite forms, can have a high strength and stiffness that are maintained to the temperatures well above 2000 °C under non-oxidative conditions.¹ However, their high temperature applications are limited to the inert atmosphere or short-term exposure, as carbon is susceptible to rapid oxidation in the air at the temperatures above about 400 °C, resulting in a considerable deterioration in their mechanical properties.² Therefore, a number of oxida-

tion-protection methods have been proposed to solve the problem and extend the service life of carbon materials. Conventional protection methods rely on refractory oxide-forming coatings as oxygen diffusion barriers on the materials, e.g., carbon fibers. This approach is only partially successful since the coatings crack during thermal cycling due to a thermal-expansion mismatch between the coating and the substrate unless rather complex, functionally graded systems are used.³

In order to alleviate some of the difficulties resulting from the coating microcracks, oxidation inhibitors such

as boride and silicide ceramic powders are sometimes added to the carbon matrix. Although this approach is effective in increasing a composite's overall resistance to oxidation, it is very difficult to solve the problem of homogeneous distribution of the ceramic powders in the matrix.⁴

One resultful approach to mitigating the problems of the coating and non-uniform mixing of an antioxidant powder with the matrix is to chemically dope the carbon-matrix precursor with organometallic functional groups to produce an intimate mixing of the antioxidant and the matrix.⁵ Coal-tar and petroleum pitches, due to their inherent chemical properties, mesophase formation and low melting points, appear to be promising carbon-matrix precursors for doping with the organo-derivatives of silicon and boron serving both as the source of reactive C-atoms toward SiC and B₄C and the carbon matrix. In the work reported by Czosnek,⁶ a typical coal-tar pitch was doped with polycarbosilane and, subsequently, carbonized at elevated temperatures to yield doped carbon materials with a homogeneous, nano-scale dispersion of the SiC particles. The resulting solids had improved oxidation-resistance characteristics.

In this work, silicon- and boron-doped carbon materials were synthesized via a co-pyrolysis and subsequent carbonization of the mixtures of the toluene-soluble fraction of the coal-tar pitch, polycarbosilane (as a silicon source) and pyridine borane (as a boron source). The main aim of this work was to develop carbon-alloy materials with a self-protection mechanism "built-in" the structure. The influence of the boron content and carbonization temperatures on the oxidation behavior of the C-Si and C-B-Si alloys was investigated. The anti-oxidative mechanism of the C-Si and C-B-Si alloys was discussed on the basis of the evolution of elemental compositions and morphology.

2 EXPERIMENTAL WORK

2.1 Preparation of Si and B-Si doped pitches and their derived C-Si and C-B-Si alloys

Polycarbosilane was purchased from Suzhou Ceramic Fiber Co. Ltd. in China. Henan Chemical Trade Co. Ltd. in China supplied pyridine borane, which was used without further purification. The coal-tar pitch was a generous gift from Wuhan Iron and Steel Co. Ltd. in China. The toluene-soluble fraction of the coal-tar pitch was obtained with a refluxing extraction using the toluene solvent and, subsequently, the removal of toluene with the distillation treatment. The toluene-soluble fraction of the coal-tar pitch was mixed with polycarbosilane at a mass ratio of 1:1 in the toluene solvent in a three-neck flask, and then a defined weight percent of pyridine borane was added to the solution. The mixture was stirred at room temperature for 2 h, heated to 180 °C and refluxed for 6 h under argon atmosphere. Then the mixture was slowly cooled to 120 °C. After removing the

toluene solvent from the mixture with a vacuum distillation, the toluene-soluble Si and B-Si doped pitches were finally obtained. The doped-pitch-sample designation and the corresponding chemical components of the raw materials used to prepare the sample are listed in **Table 1**.

Table 1: Chemical components of the raw materials used to prepare Si and B-Si doped pitches in mass fractions (w/w%)

Tabela 1: Kemijska sestava surovin, uporabljenih za pripravo s Si in B-Si dopirane smole v masnih deležih (w/w%)

Sample designation	Toluene-soluble fraction of coal-tar pitch (w/w%)	Polycarbosilane (w/w%)	Pyridine borane (w/w%)
B0	50.0	50.0	0
B2	42.7	42.7	14.6
B4	37.2	37.2	25.6
B6	33.0	33.0	34.0

In order to obtain C-Si and C-B-Si alloys, the doped coal-tar pitch was first semi-carbonized at 450 °C for 2 h under a 2 MPa pressure in an autoclave, and then the semi-carbonized samples were transferred to corundum crucibles and carbonized at 1000–1600 °C for 1 h in a tube furnace under a flow of argon atmosphere. The C-Si and C-B-Si alloys obtained with a carbonization at 1200 °C for 1 h of B0, B2, B4 and B6 were labeled as CB0-12, CB2-12, CB4-12 and CB6-12, respectively. The C-Si and C-B-Si alloys obtained with a carbonization at 1600 °C for 1 h of B0, B2, B4 and B6 were labeled as CB0-16, CB2-16, CB4-16 and CB6-16, respectively.

2.2 Analysis and characterization of C-Si and C-B-Si alloys

Phase compositions of C-Si and C-B-Si alloys were analyzed with X-ray diffraction (Philips X'PERT PRO MPD, made in Netherlands). The X-ray wavelength of the copper target (Cu K α) as a radiation source was 0.15406 nm. The working-tube voltage and current were 40 kV and 30 mA, respectively. The thermal gravimetric and differential scanning calorimetry (TG-DSC) analyses of the samples were done with a comprehensive thermal analyzer (NETZSCH STA499C type, produced in Germany). For each measurement, 50–90 mg of the sample was used. The sample was heated from the ambient temperature to 1500 °C at a heating rate of 5 °C min⁻¹ in dry air with a flow rate of 30 mL min⁻¹. A scanning electron microscope (TESCAN VEGA3, provided in Czech) equipped with a BRUKER 410-M energy dispersive spectrometer (EDS) was used to observe the morphology of the C-Si and C-B-Si alloys before and after the oxidation.

3 RESULTS AND DISCUSSION

3.1 Physical properties of the raw materials and Si and B-Si doped pitches

Table 2 shows physical properties of the toluene-soluble fraction of the coal-tar pitch, the Si and B-Si doped coal-tar pitches. The softening point and pyrolysis yield of the toluene-soluble fraction of the coal-tar pitch are 52.4 °C and reaction 39.5 %, respectively. After the doping with silicon heteroatoms, the softening point increases to 124.3 °C and the solid yield of 60.7 % is obtained. An addition of boron-bearing additives with 2 % boron to the above Si-doped coal-tar pitch results in a further increase in the softening point and pyrolysis yield, which may be related to the residual boron and silicon in the solid. For the B-Si doped coal-tar pitch, an increase in the softening point and pyrolysis yield is observed when increasing the boron content. However, the volatile content of the toluene-soluble fraction of the coal-tar pitch decreases from 72.5 % to 45.1 % after being doped with silicon and boron (6 % boron). The doping of the toluene-soluble fraction of the coal-tar pitch with the silicon and boron heteroatoms causes a decrease in the content of the quinoline insolubles. It is worth noting that the doped coal-tar pitches synthesized in this study are completely soluble in ordinary organic solvents, such as benzene, toluene and dimethylbenzene. Owing to their high solubility, the doped coal-tar pitches could be used as impregnating agents in the fabrication of C/C composites.

Table 2: Physical properties of the toluene-soluble fraction of the coal-tar pitch (TSP), the Si and B-Si doped coal-tar pitches

Tabela 2: Fizikalne lastnosti v toluenu topne frakcije premogove katranske smole (TSP) v premogovi katranski smoli, dopirani s Si in B-Si

Sample	Softening point ^a (°C)	Quinoline insoluble ^b (wt%)	Volatile content ^c (wt%)	Pyrolysis yield ^d (wt%)
TSP	54.2	0	72.5	39.5
B0	124.3	0.12	60.4	60.7
B2	151.6	0.39	53.6	64.1
B4	165.2	0.64	47.3	69.8
B6	183.5	0.97	45.1	71.4

a) Determined using a ring-and-ball apparatus; b) Specified in the quinoline solvent; c) Specified at 900 °C for 7 min; d) Specified at 780 °C for 40 min

3.2 XRD analysis of C-Si and C-B-Si alloys

The XRD patterns of the C-Si and C-B-Si alloys obtained with a carbonization of the Si and B-Si doped coal-tar pitches at different temperatures are shown in **Figure 1**. The diffraction peaks at $2\theta = 14.6^\circ$ and 27.8° in **Figures 1a** to **c** correspond to the cubic B_2O_3 phase (JCPDS Card No.00-006-0297), formed with a chemical reaction between a small amount of oxygen contained in polycarbosilane and borane produced by a decomposition of pyridine borane during the heat treatment. B_2O_3 has a low melting point (460 °C) and a good fluidity at a

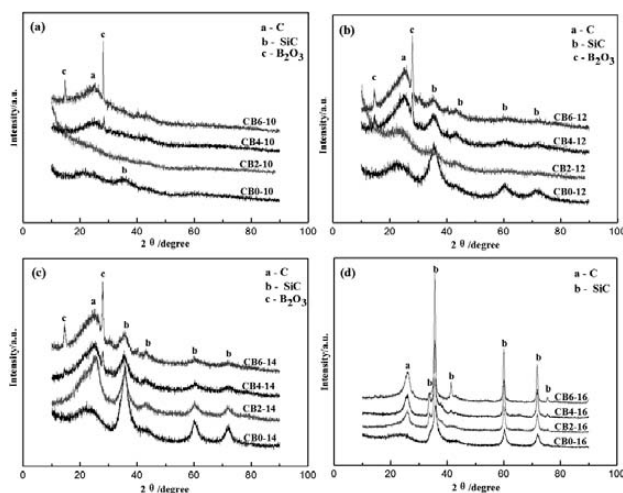


Figure 1: XRD patterns of C-Si and C-B-Si alloys obtained with a carbonization of Si and B-Si doped coal-tar pitches at: a) 1000 °C, b) 1200 °C, c) 1400 °C and d) 1600 °C for 1 h

Slika 1: XRD-posnetki zlitin C-Si in C-B-Si, dobljenih s karbonizacijjo 1 h s Si in B-Si dopirane premogove katranske smole pri: a) 1000 °C, b) 1200 °C, c) 1400 °C in d) 1600 °C

temperature above 500 °C and, as a result, it can be used as a protective glassy film covering the cracks and micropores formed during the oxidation of the carbon materials, increasing the diffusion resistance to the oxygen from the air into the carbon materials and greatly retarding the oxidation of the carbon materials. The broad and weak diffraction peaks appearing at about $2\theta = 25^\circ$ can be attributed to the (002) reflection of the pseudo-graphite carbon, which indicates a formation of the carbon with a low degree of graphitization and crystallinity in the process of carbonization. The diffraction peaks at $2\theta = (35.6^\circ, 41.4^\circ, 60^\circ, 71.8^\circ)$ in **Figures 1b** to **d** are assigned to the hexagonal β -SiC phase. Since these peaks in **Figures 1b** and **c** are broad, the SiC present in the carbon matrix formed with the carbonization treatment at 1200 °C and 1400 °C appears to be nanocrystalline. However, for the sample obtained with the carbonization treatment at 1000 °C, there is no obvious characteristic peak of the SiC phase, which shows that the SiC phase does not exist in the carbon materials or it has an amorphous structure. In addition, it can be seen from **Figure 1** that increasing the carbonization temperature to 1600 °C induces an evident increase in the relative intensity and a decrease in the full width at the half maximum (FWHM) of the characteristic peaks of the SiC, which may result from a rapid growth of the SiC crystals at a high temperature. In none of the cases did the B_4C phase occur in the carbon materials obtained with the carbonization treatment at different temperatures, which may be attributed to the non-crystalline structure of B_4C .⁷ It is worth noting that the FWHM of the diffraction peaks of the SiC phase in the Si-doped carbon materials is much lower than that of the SiC phase in the B-Si doped carbon materials when the carbonization temperature is below 1600 °C (**Figures 1a** to **c**). This implies that the grain size of the SiC in the

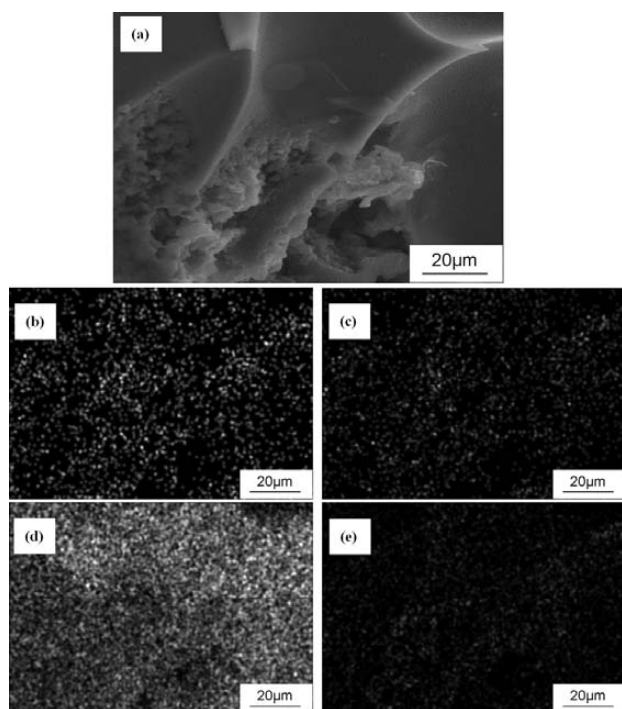


Figure 2: SEM image: a) of the C-B-Si alloy obtained with the carbonization treatment of doped coal-tar pitch B4 at 1200 °C for 1 h and the corresponding EDS elemental maps of: b) carbon, c) boron, d) silicon and e) oxygen

Slika 2: SEM-posnetek: a) zlitine C-B-Si, dobljene z 1 h karbonizacijo dopirane premogove katranske smole B4 pri 1200 °C, in EDS-posnetki razporeditve elementov: b) ogljika, c) bora, d) silicija in e) kisika

Si-doped carbon materials is larger than that of the SiC in the B-Si doped ones. When the carbonization temperature increases to 1600 °C, the diffraction peaks of B₂O₃ disappear from the carbon materials due to an intense vaporization of B₂O₃ at high temperatures. Moreover, the FWHM of the diffraction peaks of the SiC in the Si-doped carbon materials is much larger than that of the SiC in the B-Si doped ones when the carbonization temperature is 1600 °C. The converse is found in the samples obtained with the carbonization at the temperature below 1600 °C (shown in **Figures 1a** to **c**). The possible reasons still need to be further studied.

Figure 2a shows the typical morphology of the C-B-Si alloy obtained with the carbonization treatment of doped coal-tar pitch B4 at 1200 °C for 1 h. It can be seen that the resulting C-B-Si alloy is composed of many polycrystalline grains. The corresponding maps of carbon, boron, silicon and oxygen elemental distributions are shown in **Figures 2b** to **e**, revealing that carbon, boron and silicon are uniformly distributed in the alloy materials.

3.3 Oxidation behavior analysis of the C-Si and C-B-Si alloys

To investigate the influences of the pyridine-borane content in raw materials and carbonization temperatures on the oxidation resistance of the resulting C-Si and

C-B-Si alloys, the C-Si and C-B-Si alloys obtained with the carbonization treatment of B0, B2, B4 and B6 at 1200 °C and 1600 °C were put into a tube furnace, heated from room temperature to 1000 °C and kept for 1–10 h in air. The oxidation weight loss as a function of time of the C-Si and C-B-Si alloys is shown in **Figure 3**. It can be seen from **Figure 3a** that the oxidation weight loss of sample CB0-12 tends towards stability when the oxidation time exceeds 3 h. After being oxidized at 1000 °C for 10 h, its oxidation weight loss is about 10 %. On the other hand, the weight loss of samples CB2-12, CB4-12 and CB6-12 increases gradually with the prolonged oxidation time. The difference in the weight loss between the three samples is gradually diminishing. After the oxidation for 10 h, the weight losses for the three samples are very close (about 6 %). Obviously, in the case of the C-Si and C-B-Si alloys prepared with the carbonization treatment at 1200 °C, the oxidation resistance of the former is inferior to that of the latter under the same oxidation conditions. When increasing the carbonization temperature to 1600 °C, the oxidation resistances of the resulting C-Si and C-B-Si alloys drop

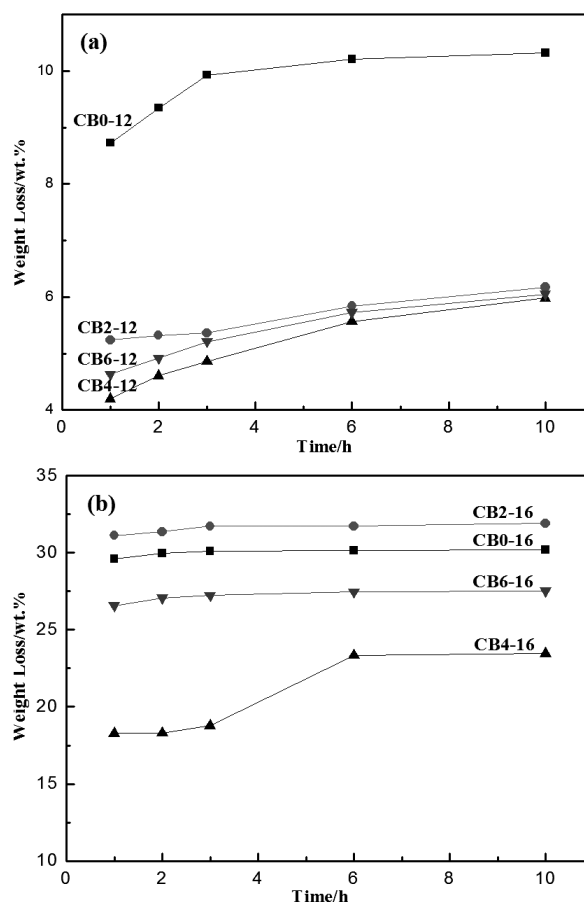


Figure 3: Oxidation weight loss at 1000 °C in the air as a function of time for the C-Si and C-B-Si alloys obtained with the carbonization treatment of B0, B2, B4 and B6 at: a) 1200 °C and b) 1600 °C for 1 h

Slika 3: Izguba mase pri oksidaciji na 1000 °C na zraku v odvisnosti od časa pri zlitinah C-Si in C-B-Si, dobljenih s karbonizacijo B0, B2, B4 in B6 1 h na: a) 1200 °C in b) 1600 °C

sharply, which can be discerned from the comparison of **Figures 3a** and **b**. After the oxidation for 10 h, the weight losses of samples CB0-16, CB2-16, CB4-16 and CB6-16 obtained with the carbonization at 1600 °C are 30 %, 32 %, 23 % and 27 %, respectively, being much higher than those of the corresponding alloys obtained with the carbonization at 1200 °C. The above results of the oxidation resistance indicate that adjusting the content of pyridine borane in the raw materials in the synthesis of the B-Si doped coal-tar pitch and selecting the appropriate carbonization temperature in the following carbonization stage play an important role in improving the oxidation resistance of the obtained C-B-Si alloy.

Figure 4 shows the XRD patterns of the C-Si and C-B-Si alloys kept in air at 1000 °C for 3 h. For the C-B-Si alloys obtained with the carbonization treatment at 1200 °C, there is no evident difference between the XRD patterns before and after their oxidation in the air (**Figures 1b** and **4a**) and the broad diffraction peak at $2\theta = 25^\circ$ assigned to carbon (**Figure 4a**) is still distinct, suggesting the existence of the residual carbon in the oxidation products of CB2-12, CB4-12 and CB6-12. However, for the C-Si alloy obtained with the

carbonization treatment at 1200 °C, there is a dramatic drop in the diffraction-peak intensity of the SiC after its oxidation in the air (**Figures 1b** and **4a**) and a broad diffraction peak appears at $2\theta = 22^\circ$, which can be attributed to the SiO₂ formed due to the oxidation of the SiC. **Figure 4b** shows the XRD patterns of the oxidation products of the C-Si and C-B-Si alloys obtained with the carbonization treatment at 1600 °C. It can be seen from **Figures 1d** and **4b** that the diffraction peak at $2\theta = 25^\circ$ assigned to the carbon in the C-Si and C-B-Si alloys disappears from their corresponding oxidation products, as a result of the burning up of the carbon during the oxidation of the C-Si and C-B-Si alloys. On the other hand, a very strong diffraction peak at $2\theta = 22^\circ$ assigned to the SiO₂ phase occurs in the oxidation product of the C-Si alloy. The above XRD analysis of the oxidation products indicates that the C-B-Si alloy obtained with the carbonization treatment at 1200 °C has a better oxidation resistance than those obtained with the carbonization treatment at 1600 °C. This fact can be explained with the difference in the grain sizes of the SiC and B₄C in the C-B-Si alloy formed at different carbonization temperatures. The higher the carbonization temperature, the larger is the SiC grain size in the C-B-Si alloy. Large SiC grains are difficult to oxidize and, as a result, there is no continuous protective oxide film formed on the surface of the C-B-Si alloy during the air oxidation at 1000 °C. Oxygen from the air diffuses into the interior of the C-B-Si alloy through the cracks and holes and then reacts with carbon, which leads to a continuous combustion of carbon. However, small SiC grains are susceptible to oxidation. The SiO₂ formed with the oxidation of the SiC has a good fluidity at 1000 °C, thus forming a continuous protective oxide film sealing the microcracks and micropores in the C-B-Si alloy,⁸ retarding the diffusion of the oxygen and decreasing the oxidation rate of the carbon.

In order to further understand the influence of the pyridine-borane content in the raw materials on the oxidation behavior of the C-Si and C-B-Si alloys, the morphology and structure of the C-Si and C-B-Si alloys before and after the oxidation in the air at 1000 °C for 3 h was observed with SEM. As shown in **Figure 5a**, the C-Si alloy possesses a loose structure and there are many micro-holes on its surface. Oxygen from the air diffuses into the interior through these micro-holes and reacts with the carbon in the C-Si alloy during oxidation, leading to a continuous weight loss of the C-Si alloy, as can be seen from **Figure 3a**. After the oxidation in the air at 1000 °C for 3 h, the micro-holes on the surface disappear and a smooth glassy film is formed (**Figure 5b**). The EDS spectrum of the oxidation product of CB0-12 shows that it is mainly composed of oxygen and silicon. The EDS spectrum and the above XRD analysis indicate that the main component of the glassy film is the non-crystalline SiO₂. This protective glassy film restrains the diffusion of oxygen to a great extent, and, as a result,

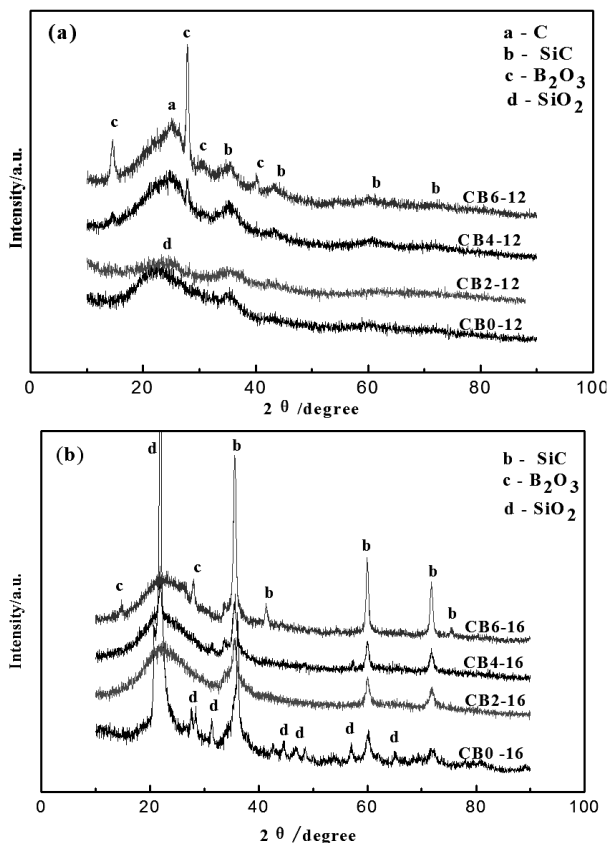


Figure 4: XRD patterns of the oxidation products of the C-Si and C-B-Si alloys in air at 1000 °C for 3 h. The C-Si and C-B-Si alloys are obtained with the carbonization treatment at: a) 1200 °C and b) 1600 °C for 1 h.

Slika 4: XRD-posnetki oksidacijskih produktov po žarenju zlitin C-Si in C-B-Si 3 h na 1000 °C. Zlitine C-Si in C-B-Si so bile dobljene s karbonizacijo 1 h pri: a) 1200 °C in b) 1600 °C.

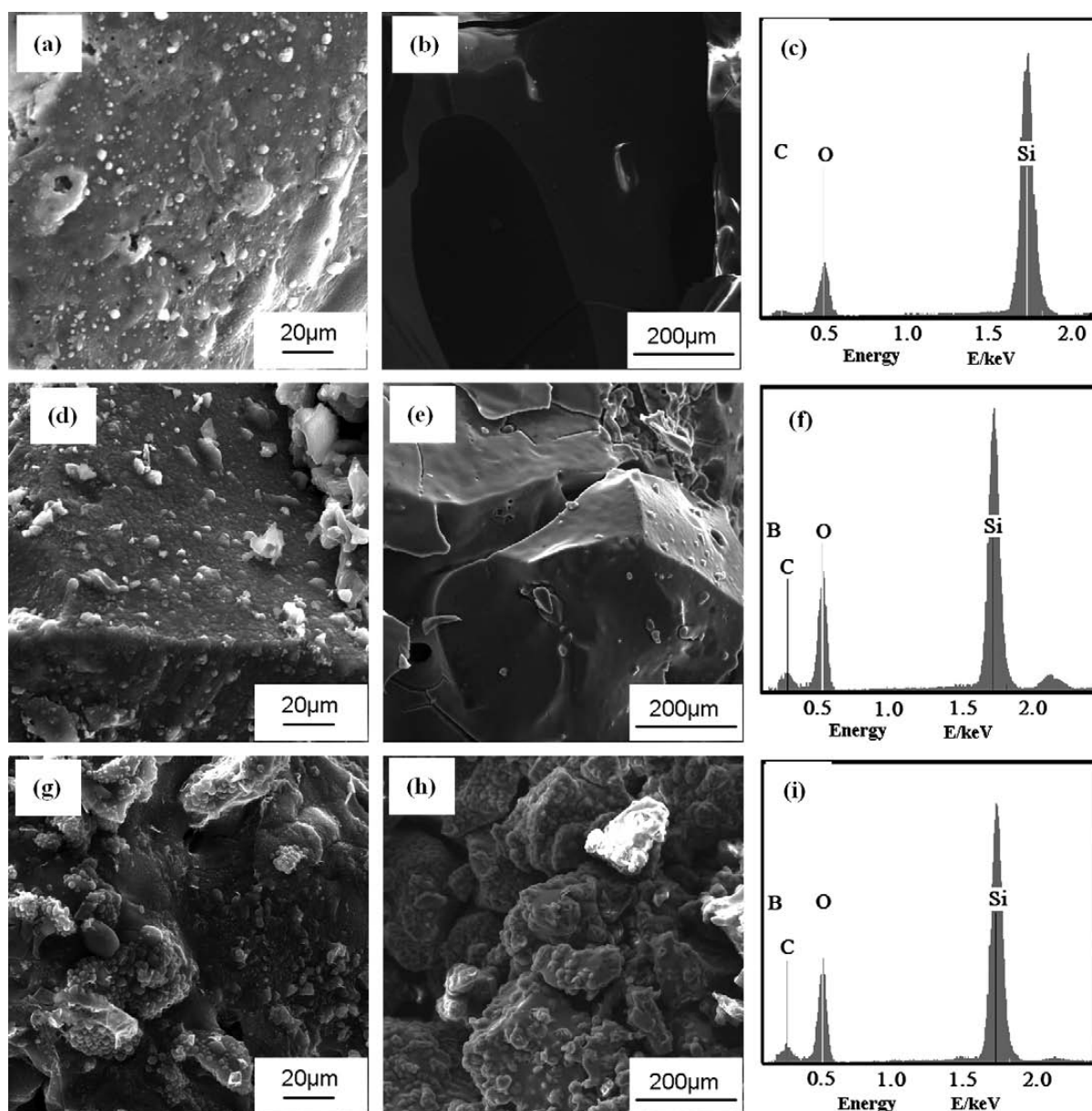


Figure 5: Typical SEM images of CB0-12, CB4-12 and CB6-12: a), c), e) before and b), d), f) after the oxidation in the air at 1000 °C for 3 h. EDS spectra of: c) CB0-12, f) CB4-12 and i) CB6-12 after the oxidation, corresponding to b), e) and h), respectively.

Slika 5: Značilni SEM-posnetki CB0-12, CB4-12 in CB6-12: a), c), e) pred oksidacijo in b), d), f) po njej 3 h na zraku na 1000 °C. EDS-spektri c) CB0-12, f) CB4-12 in i) CB6-12 po oksidaciji ustrezajo b), e) in h).

CB0-12 tends towards a constant weight loss after the oxidation for 3 h at 1000 °C (**Figure 3a**). Unlike sample CB0-12, sample CB4-12 has a relatively dense structure, as shown in **Figure 5d**. The formation of a dense structure may benefit from the sintering-aiding action of the B_2O_3 in sample CB4-12 (**Figure 1b**), which is commonly used as a flux former and can reduce the sintering temperature to obtain dense ceramics.^{9,10} Moreover, the presence of B_2O_3 is beneficial for retarding the oxidation of the carbon in sample CB4-12 in the temperature range of 450–850 °C, as B_2O_3 has a low viscosity and a good mobility in this temperature range, therefore sealing the microcracks.¹¹ However, in the temperature range of

450–850 °C, the SiO_2 formed with the oxidation of the SiC in sample CB4-12 does not possess the function of sealing the microcracks so that no protective SiO_2 film can be formed in a short time because of its high viscosity and poor fluidity. These factors explain why the weight loss of sample CB4-12 is much lower than that of CB0-12 under the same oxidation conditions. After the oxidation for 3 h at 1000 °C, a continuous glassy film is formed on the surface of sample CB4-12, containing silicon, oxygen, carbon and boron (**Figure 5f**), consistent with the XRD pattern of the oxidation product of CB4-12 shown in **Figure 4a**. The SiO_2 formed with the oxidation of the SiC might be soluble in liquid B_2O_3

forming liquid borosilicate, which exists in the form of a B_2O_3 - SiO_2 eutectic solution. The borosilicate glass has a much lower volatility and oxygen permeability so that it can inhibit the volatilization of the B_2O_3 and an oxidation of the carbon substrate. These synergistic oxidation-resistance effects have also been reported by Li et al.^{12,13} The glassy film on sample CB4-12 is not perfect, however, there are some pinholes on its surface (Figure 5e), acting as diffusion channels for the oxygen from the air, resulting in a continuous oxidation of the carbon and a slow increase in the weight loss of sample CB4-12 (Figure 3a). The pyridine-borane content in the raw materials used for preparing sample CB6-12 is larger than that used for sample CB4-12. A structure comparison between CB4-12 and CB6-12, shown in Figures 5d and g, respectively, implies that a high pyridine-borane content in the raw materials is unfavorable for the formation of a dense structure during the preparation of the C-B-Si alloy. The microcracks and holes in sample CB6-12 act as diffusion channels for the oxygen from

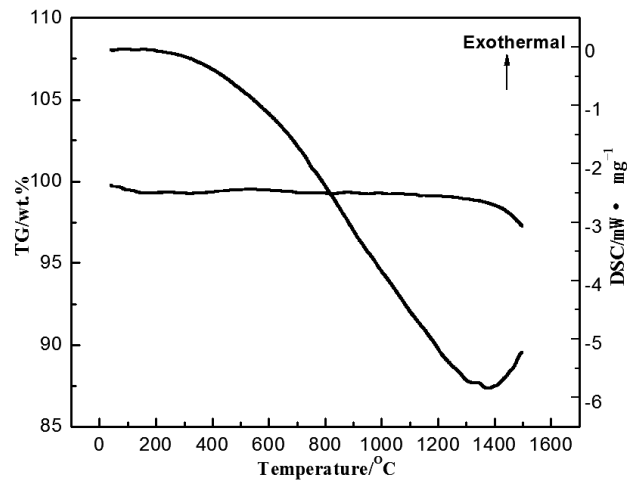


Figure 7: TG-DSC curve of CB4-12 in a dry-air flow at a heating rate of 5 °C/min

Slika 7: TG-DSC-krivulja za CB4-12 pri pretoku suhega zraka in hitrosti ogrevanja 5 °C/min

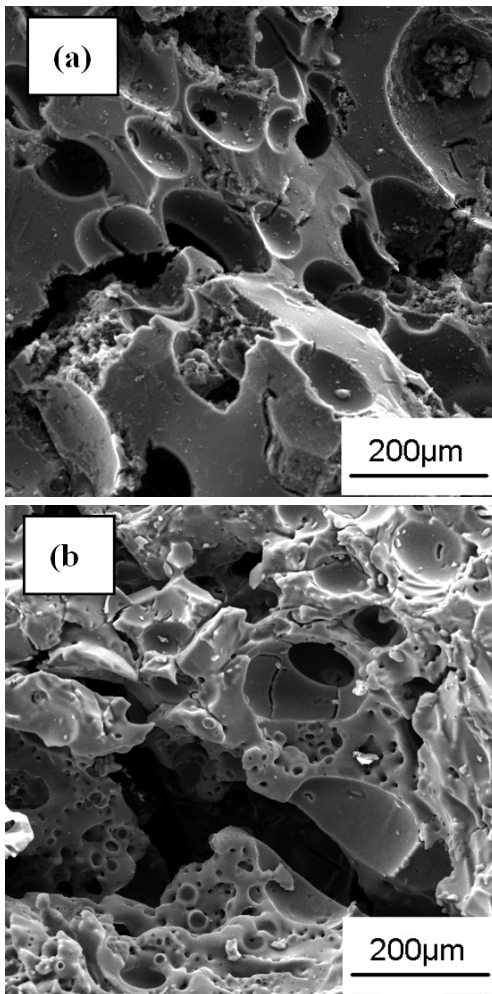


Figure 6: Typical SEM images of CB4-16: a) before and b) after the oxidation in the air at 1000 °C for 3 h

Slika 6: Značilna SEM-posnetka CB4-16: a) pred in b) po oksidaciji 3 h na zraku na 1000 °C

the air during the oxidation, causing a higher weight loss of CB6-12 than in the case of CB4-12 under the same oxidation conditions. After the oxidation for 3 h at 1000 °C, a discontinuous glassy film with the same element composition (Figure 5i) as the film shown in Figure 5f is formed on sample CB6-12 and many coarse particles are exposed outside the film. It can be expected that as the oxidation time increases, the thickness of the glassy film will gradually increase, and the coarse particles will finally be completely covered.

Figure 6 shows typical SEM images of CB4-16 before and after the oxidation in the air at 1000 °C for 3 h. As can be seen from Figure 6a, CB4-16 has a loose and porous structure, which is quite different from the dense structure of CB4-12 (Figure 5d). The loose and porous structure may result from an intense volatilization and escaping of B_2O_3 during the preparation of CB4-16, whose boiling point is 1500 °C at atmospheric pressure. The SEM observations indicate that too high a carbonization temperature (>1500 °C) is unfavorable for the formation of a dense structure for the C-B-Si alloy. Furthermore, the higher the carbonization temperature, the larger is the grain size of the SiC in C-B-Si alloys.¹⁴ The growth of the SiC grains induces an increase in the initial oxidation temperature,¹⁵ which can be confirmed with the abundance of the remaining SiC phase in the oxidation product of CB4-16 (Figure 4b). The volatilization loss of the B_2O_3 and the increase in the initial oxidation temperature of the SiC in CB4-16 make it very difficult to form a protective glassy film and, as a result, a great deal of carbon is oxidized. This explains the fact why the weight loss of sample CB4-16 is much higher than that of sample CB4-12 under the same oxidation conditions. After the oxidation at 1000 °C for 3 h, a large number of honeycomb-like holes occur in sample CB4-16, which may be left over during the escape of the CO and CO_2 formed by the oxidation of carbon. The

above SEM observations for sample CB4-16 agree with the oxidation-weight-loss curves shown in **Figure 3b**, further confirming that the oxidation resistance of CB4-16 is inferior to that of CB4-12.

To have a better insight into the dynamic oxidation behavior of the C-B-Si alloys, the TG-DSC analysis of CB4-12 was carried out on a comprehensive thermal analyzer, as shown in **Figure 7**. As the temperature increases from room temperature to about 150 °C, the mass of the sample decreases gradually and the weight loss is about 1 % when the temperature reaches about 150 °C. The weight loss in this temperature range may result from the volatilization of the moisture absorbed in the sample. In the temperature range of 150–300 °C, there is no obvious mass change, exhibiting the sample's good antioxidant ability. However, when the temperature is over 1400 °C, the mass of the sample decreases significantly, which could be attributed to a fast gasification of the protective glassy film composed of SiO₂ and B₂O₃ at a high temperature in the flowing air.¹⁶ In addition, a strong exothermic peak appears at the temperature close to 1400 °C on the DSC curve, indicating a rapid and violent oxidation of the carbon in the C-B-Si alloy.

4 CONCLUSIONS

The solvent-soluble Si and B-Si doped coal-tar pitches were synthesized with the co-pyrolysis of a mixture of the toluene-soluble fraction of the coal-tar pitch, polycarbosilane and pyridine borane. The softening point and the pyrolysis yield of the doped coal-tar pitch increase with the increasing of the content of pyridine borane in the raw materials. The C-B-Si alloy composed of SiC, B₂O₃ and C can be obtained with the carbonization treatment of the synthetic B-Si doped coal-tar pitch at high temperatures. The boron content and the carbonization temperature have significant influences on the oxidation resistance of the resulting alloys. In most cases, the oxidation resistance of the C-B-Si alloy is better than that of the C-Si alloy, which can be attributed to the sintering-aiding action of B₂O₃ and the anti-oxidation synergism of the SiO₂ and B₂O₃ formed during the oxidation. The higher the carbonization temperature, the larger is the grain size of the SiC in the C-B-Si alloy. A large grain size leads to an increase in the initial oxidation temperature of the SiC, which is unfavorable for the formation of a protective glassy film on the surface of the C-B-Si alloy. As a result, after the oxidation at 1000 °C for 10 h, the weight loss of CB4-12 is less than 6 %, whereas it is 23 % for CB4-16. In view of the excellent oxidation resistance of CB4-12 derived from the B-Si doped coal-tar pitch, the B-Si doped pitches synthesized in this study can be used as promising impregnating agents in the fabrication of car-

bon/carbon composites, so as to increase their oxidation resistance at high temperatures.

Acknowledgements

This work was financially supported by the National Natural Science Foundation of China (91016003, 51352001) and Scientific Research Fund of Hubei Provincial Education Department (Q20104403).

5 REFERENCES

- S. Lu, B. Rand, K. D. Bartle, et al., Novel oxidation resistant carbon-silicon alloy fibres, *Carbon*, 35 (1997), 1485–1493
- A. V. K. Westwood, R. Brydson, R. Coult, et al., Carbon-boron-nitrogen alloys from borazarene-derived mesophase pitches, *Carbon*, 40 (2002), 2157–2167
- A. V. K. Westwood, B. Rand, S. Lu, Oxidation resistant carbon materials derived from boronated carbon-silicon alloys, *Carbon*, 42 (2004), 3071–3080
- C. F. Wang, F. R. Huang, Y. Jiang, et al., Oxidation behavior of carbon materials derived from a carborane- and silicon-incorporated polymer, *Ceramics International*, 38 (2012), 3081–3088
- P. P. Partha, T. S. Stuart, Carbon materials obtained from organometallic modification of pitch and its oxidation resistance properties, *Carbon*, 34 (1996), 89–95
- C. Czosnek, W. Ratuszek, J. F. Janik, et al., XRD and ²⁹Si MAS NMR spectroscopic studies of carbon materials obtained from pyrolyses of a coal tar pitch modified with various silicon-bearing additives, *Fuel Processing Technology*, 79 (2002), 199–206
- A. V. K. Westwood, B. Rand, S. Lu, Oxidation resistant carbon materials derived from boronated carbon-silicon alloys, *Carbon*, 42 (2004), 3071–3080
- J. Y. Liu, F. Li, J. Liu, et al., Micro-analysis of high-temperature oxidation-resistance of a new kind of heat-resistant grid plate in grate-kiln, *International Journal of Minerals, Metallurgy and Materials*, 16 (2009) 6, 632–639
- K. K. Chang, L. Jiang, D. L. Mao, et al., Photoluminescence of 4SrO7Al₂O₃ ceramics sintered with the aid of B₂O₃, *Ceramics International*, 30 (2004), 285–290
- H. P. Wang, S. Q. Xuy, S. Y. Zhai, et al., Effect of B₂O₃ additives on the sintering and dielectric behaviors of CaMgSi₂O₆ ceramics, *Journal of Materials Science and Technology*, 26 (2010) 4, 351–354
- Y. Q. Li, T. Qiu, Oxidation behavior of boron carbide powder, *Materials Science and Engineering A*, 444 (2007), 184–191
- J. Li, R. Y. Luo, C. Lin, et al., Oxidation resistance of a gradient self-healing coating for carbon/carbon composites, *Carbon*, 45 (2007), 2471–2478
- N. Takayuki, G. Takashi, M. Makoto, et al., Oxidation of boron carbide-silicon composite at 1073 K to 1773 K, *Materials Transactions*, 44 (2003) 3, 401–406
- T. Sogabe, T. Matsuda, K. Kuroda, et al., Preparation of B₄C-mixed graphite by pressureless sintering and its air oxidation behavior, *Carbon*, 33 (1995), 1783–1788
- T. Eichner, M. Braun, K. J. Huttinger, Element-substituted polyaromatic mesophases: I. Boron-substitution with the pyridine-borane complex, *Carbon*, 34 (1996), 1367–1381
- Z. J. Fan, Y. Z. Song, Oxidation behavior of fine-grained SiC-B₄C/C composites up to 1400 °C, *Carbon*, 41 (2003), 429–436